EPSC Abstracts
Vol. 10, EPSC2015-28, 2015
European Planetary Science Congress 2015

Geometry of the intermediate transition in the Venus plasma wake

H. Pérez-de-Tejada (1), R. Lundin (2), , M. Reyes-Ruiz (3), H. Durand-Manterola (1), S. Barabash (2), T. L. Zhang (4), J. A., Sauvaud (5); (1) Institute of Geophysics, UNAM, México, D. F; (2) Swedish Institute of Space Physics, Kiruna, Sweden; (3) Institute of Astronomy, UNAM, Ensenada, México; (4) Space Research Institute, Graz, Austria; (5) CESR, Toulouse, France.

ABSTRACT

The ASPERA plasma data and the magnetic field measurements of the Venus Express lead to the observation of the intermediate transition as the spacecraft approached the planet through the Venus wake. An analysis was conducted on data obtained in 4 different observation periods between 2006 and 2009 when that transition occurred by the midnight plane. A data set plotted on the YZ plane transverse to the solar wind direction indicates that the intermediate transition spreads out away from the wake with the downstream distance from the planet and that its displacement is more noticeable on a direction transverse to the ecliptic plane.

VEX DATA

A selection of Venus Express orbits was made in each observation period for the orbit that is traced closest to the midnight plane and thus that can provide a better identification of the intermediate transition which arises from momentum transport processes by the polar regions. An example of the energy spectra of the solar wind and the planetary O+ ions, together with their density and speed profiles derived from those spectra in the 27-08-2008 orbit is shown in Figure 1. Among the various features seen in the energy spectra in that figure it is noticeable the strong change that occurs in the energy spectrum of the H+ ions (top panel) at 03:23 UT with a gradual energy decrease before that time and a severe absence of ion fluxes right afterwards. At that time there is a sudden drop in the density and speed of those ions similar to what has been reported across a plasma transition in previous studies (1). Equally notable is an increase of the solar wind ion density and magnetic field intensity measured by 02:00UT as the spacecraft moved along the wake and that is comparable to a bow shock crossing far downstream from Venus (at X ~3.69 R_V). Figure 1 also shows that throughout its transit through the Venus wake the Venus Express moved near the midnight plane since there are only very small values of the Y coordinate. Independent of those measurements in the wake an outbound bow shock crossing upfront at ~04:15 UT was also detected.

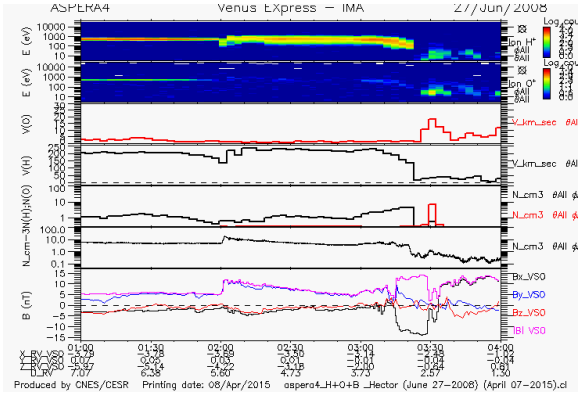

Figure 1. Energy spectra of the solar wind and planetary O+ ions measured with the Venus Express spacecraft in the Venus wake on August 27, 2008.

Together with the example shown in Figure 1 we selected 4 orbits between 2006 and 2009 that are traced in the vicinity of the midnight plane. Those cases are listed in Table I with the time and the coordinate values where the intermediate transition and the inbound bow shock were detected. The X and the Z coordinate values of both transitions in the 4 observation periods are plotted separately in Figure 2 in different data sets. Both of them show a similar trend with the X and Z values reaching a smaller (negative) magnitude in the later orbits (27-06-2008 and 19-09-2009). However, while there is a nearly linear variation in the position of the bow shock between 2006 and 2009 a similar dependence seems to be applicable to the data points of the early orbits (23-08-2006 and 17-11-2007) for the intermediate transition. In fact, in the 2 latter orbits (27-06-2008 and 19-09-2009), the position of the data points of the intermediate transition taper off along the X-direction suggesting that its shape may be modified in the near Venus wake (at smaller X values).

A further analysis of the position of the intermediate transition in the September-2009 observation period was conducted by selecting 12 orbits of the Venus Express where the spacecraft probed throughout the inner wake Different from the small values of the Y coordinate indicated in Table 1 the Y values in the 12 orbits now extend between ± 0.50 R_V for the 12 orbits.

The position of the intermediate transition derived from these orbits is plotted in Figure 3 to show a near linear dependence between their X and Z coordinate values. That variation indicates that with larger X distances downstream from Venus the intermediate transition becomes located further away from the wake as it is also indicated in Figure 2,

	INTERMEDIATE TRANSITION		BOW SHOCK		
	23-08-06	17-11-07		23-08-06	17-11-07
UT	01:36	00:48	UT	00:00	23:28
X	-3.23	- 3.00	X	-4.26	-3.88
Y	0.02	0.10	Y	0.02	0.19
Z	-1.44	-1.35	Z	-4.48	-4.35

	INTERMEDIATE TRANSITION		BOW SHOCK		
	27-06-08	19-09-09		27-06-08	19-09-09
UT	03:22	01:47	UT	02:00	00:38
X	-2.68	-2.56	X	-3.69	-3.30
Y	-0.03	0.04	Y	0.03	0.02
Z	-1.00	-1.18	Z	-4.22	-4.00

TABLE I. Date and time (in UT) together with coordinate values (in Venus radii) for the position of Venus Express at the intermediate transition and at the inbound Venus bow shock that were detected in 4 orbits traced by the midnight plane at different observation periods.

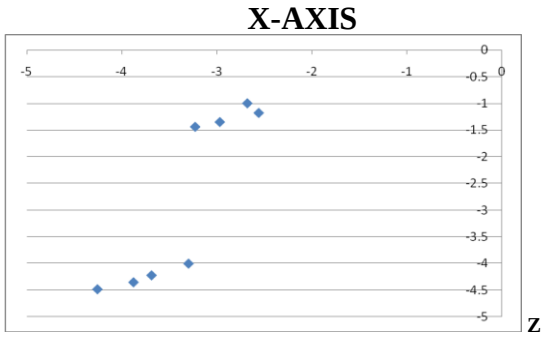

Figure 2. Data points for the intermediate transition (upper set) and for the bow shock (lower set) of the 4 orbits of Table I traced on the XZ plane .

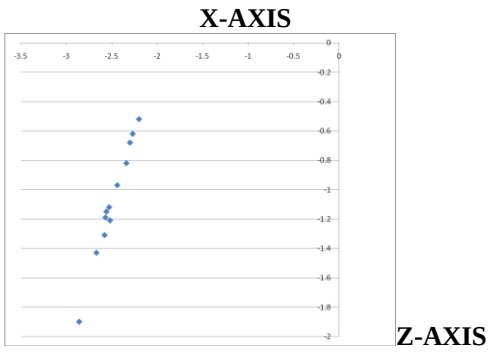

Figure 3. Data points for the intermediate transition derived from 12 orbits of the Venus Express that probed around the midnight plane between 12-09-09 and 26-09-09 in the September 2009 observation period.

DISCUSSION

The overall tendency for the intermediate transition and the bow shock to be located at smaller X and Z coordinate values in the later observation periods between 2006 and 2009 as shown in Figure 2 is consistent with the onset of solar minimum conditions by 2009 when the ionospheric plasma becomes less eroded by the solar wind. Even though the response in the position of both transitions is consistent with that variation the same issue was also addressed by comparing the position of the intermediate transition in 12 selected orbits between 12-09-09 and 26-09-09 that probed throughout the inner wake in the September-2009 observation period. The results in Figure 3 show a near linear dependence between the Z and the X-coordinate values in the position of the intermediate transition, thus indicating that even in the same observation period the displacement of that transition away from the wake along the Z-coordinate increases downstream from the planet. In fact, the interaction between the solar wind and the upper polar ionosphere is different from that at other latitudes as plasma channels are produced by the polar regions (2) thus expanding the eroded upper ionosphere into the wake. Such conditions are different further downstream where the expansion process mostly proceeds away from the wake (1).

[1] Pérez-de-Tejada, H. et al., JGR, 116, doi:JA015216, 2011.
[2] Pérez-de-Tejada, H. et al., JGR, 109, doi:JA009811, 2004.

EPSC Abstracts
Vol. 10, EPSC2015-125, 2015
European Planetary Science Congress 2015

The role of Io in the dynamics of Jupiter's magnetosphere: A sandpile modelling approach.

J.J. Reed (1), C. M. Jackman (1) and M.P. Freeman (2)
(1) University of Southampton, United Kingdom, (2) British Antarctic Survey, United Kingdom

(jr1e13@soton.ac.uk, C.Jackman@soton.ac.uk, mpf@bas.ac.uk)

Abstract

Jupiter's magnetosphere is thought to be largely internally driven, by the combination of the loading of ~500 kg/s of plasma into the system by the volcanic moon Io, and the rapid rotation of the planet itself. Since we do not see a continuously expanding torus and magnetosphere, we would expect a long-term balance between the inflow of mass, primarily from Io, and the outflow of mass, via plasmoid release.
Simple calculations, which attempt to match the mass-loading rate from Io with the amount of mass lost via large-scale tail reconnection events, indicate a significant mass imbalance at Jupiter. This mass imbalance may be due to several reasons, including visibility issues linked to single spacecraft observations.
This is where modelling can be a powerful tool. A single spacecraft can only expect to observe a global 'systemwide' event, where energy is redistributed across the entire system, with any certainty. While 'internal' events, with a more local redistribution of energy, are likely to be missed. Using computational modeling we are able to 'observe' an entire system at any time. Cellular automata (CA) based on robust physical parameters and rules can allow us to manipulate the inputs and drivers of magnetotail physics, and to explore the response of the system over a range of temporal and spatial scales. Here we examine the variability of the mass-loading and the response of our CA sandpile model to an analogous driving. We explore whether Jupiter's magnetospheric dynamics can be explained purely in terms of Io mass-loading. In particular we examine the difference between the small local events ("internal" avalanches) and larger global events ("systemwide" avalanches), and what this can tell us about the fate of mass in Jupiter's magnetosphere.

EPSC Abstracts
Vol. 10, EPSC2015-149, 2015
European Planetary Science Congress 2015

Statistical Study of Plasma-depleted Flux Tubes in Saturnian Magnetosphere

H.R. Lai (1), C.T. Russell (1), H.Y. Wei (1), M.K. Dougherty (2), and Y.D. Jia (1)
(1) Department of Earth, Planetary and Space Sciences, University of California, Los Angeles, USA (hlai@igpp.ucla.edu) (2) Imperial College London, The Blackett Laboratory, London, UK

Abstract

We have surveyed the occurrence of flux tubes with both enhanced and depressed field strength relative to their surroundings as observed in Cassini magnetometer data. Consistent with earlier studies, enhanced field flux tubes are concentrated near the equator while depressed field flux tubes are distributed in a larger latitudinal region. For both types of flux tubes, their occurrence rates vary with the local time in the same pattern and they contain the same magnetic flux. Therefore, we suggest that those two types of tubes are just different manifestations of the same phenomenon. Near the equator with high ambient plasma density, the flux tubes convecting in from the tail are compressed, resulting in increased field strength. Off the equator, these flux tubes expand slightly, resulting in decreased field strength. The enhanced flux tubes gradually break into smaller ones as they convect inward. Inside an L value of about 5, they become indistinguishable from the background.

1. Introduction

Every second, 100s of kilograms of water group neutrals and plasma are added to the Saturnian magnetosphere from Enceladus. The newly added plasma is accelerated to the rotational speed of the planet and convects outward. The plasma is lost through magnetic reconnection in the tail. The 'empty' reconnected magnetic flux must return from the tail back to the inner magnetosphere in steady state. In early studies [e.g., 1 and 2], flux tubes with both enhanced and depressed field strength relative to their surroundings have been detected. However, the relationship between the two types of phenomena is unclear. Here we have systematically surveyed all the available 1-sec magnetic field data measured by Cassini and use the statistical properties of the flux tubes to improve our understanding.

2. Statistical Properties

We select all the flux tubes distinguishable from their neighbours by a difference in field strength detected inside 15 Saturn radii and lasting from 30 seconds to 15 minutes. As Figure 1 shows, the enhanced field flux tubes are concentrated in a latitudinal and L-shell region where the surrounding plasma density is high; while the depressed flux tubes are distributed in a larger latitudinal and L-shell region. Figure 2 shows that the occurrences of both types of flux tubes vary with the local time in the same pattern.

If we assume the cross section of the flux tube is a circle and the diameter is the product of duration and rotational speed, we can estimate the flux contained in each flux tube. Here we employ 10km/s as the speed at the surface of equator. As Figure 1 shows, the medians of magnetic flux contained in both types of flux tubes are the same.

We further classify the enhanced flux tubes, which are much easier to identify, into four different groups based on their shapes. Figure 3 shows the occurrence ratio of different types as a function of L-shell number. We can see that simple and single flux tubes are more frequently observed when the L-shell number increases while complex and clustered flux tubes are more frequently observed when the L-shell number decreases.

3. Figures

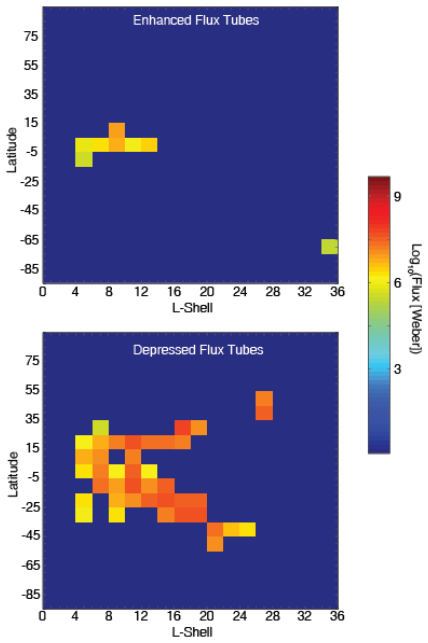

Figure 1. Medians of magnetic flux contained in enhanced (upper) and depressed (lower) flux tubes.

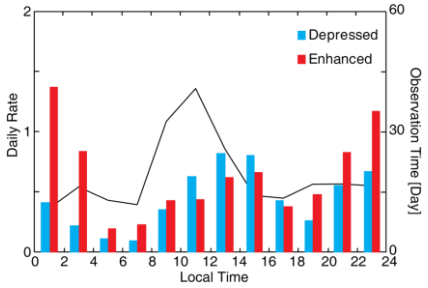

Figure 2: Daily rate of enhanced and depressed flux tubes as a function of local time.

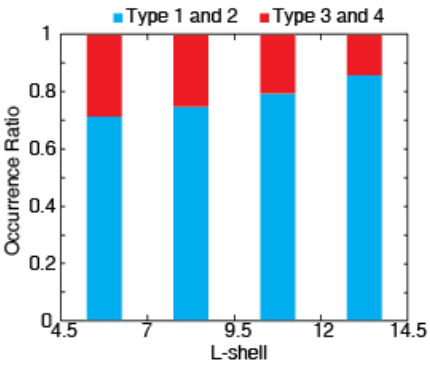

(a)

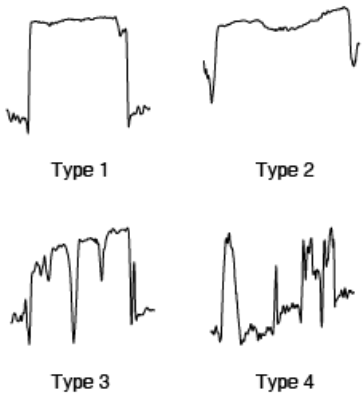

(b)

Figure 3: Occurrence ratio (a) of different types (b) of enhanced flux tube as a function of L-shell.

4. Summary and Conclusions

Based on the flux estimation and the occurrence variation with local time, we suggest that both enhanced and depressed flux tubes are the same phenomenon detected at different plasma conditions. Near the equator in the range of the E region torus, where the ambient plasma density is high, the flux tubes are compressed and field strength increases; while when the ambient plasma density is low off the equator, the flux tubes slightly expand and the field strength decreases. As the enhanced flux tubes convect inward, they break into smaller flux tubes and disappear inside L value of about 5.

References

[1] Russell, C.T., Leisner, J.S., Arridge, C.S., Dougherty, M.K., and Blanco-Cano, X.: Nature of magnetic fluctuations in Saturn's middle magnetosphere, J. Geophys. Res., 111, A12205, doi: 10.1029/2006JA011921, 2006.

[2] Andre, N., et al., Magnetic signatures of plasma-depleted flux tubes in Saturnian inner magnetosphere, Geophys. Res. Lett., 34, L14108, doi: 10.1029/2007GL030374, 2007.

EPSC Abstracts
Vol. 10, EPSC2015-157, 2015
European Planetary Science Congress 2015

Remote observation of Jupiter's magnetosphere by EXCEED on Hisaki spacecraft

K. Yoshioka (1), G. Murakami (2) , T. Kimura (3) , H. Tadokoro (4) , C. Tao (5) , M. Kagitani (6) , F. Tsuchiya (6) , A. Yamazaki (2) , T. Sakanoi (6) , Y. Kasaba (6) , I. Yoshikawa (7) , and M. Fujimoto (2,8)
(1) Rikkyo University, Tokyo, Japan, (2) ISAS/JAXA, Kanagawa, Japan, (3) Riken, Saitama, Japan, (4) Musashino University, Tokyo, Japan, (5) IRAP, Université de Toulouse/UPS-OMP/CNRS, Toulouse, France, (6) Tohoku University, Miyagi, Japan, (7) The University of Tokyo, Chiba, Japan (8) Tokyo institute of Technology, Tokyo, Japan, (kazuo@rikkyo.ac.jp)

Abstract

Hisaki is the space-telescope dedicated for planetary science. It was launched in September 2013 and orbiting around the Earth with its altitude of around 1000 km (orbital period is 106 minutes) [1]. Since December 2013, the spacecraft is observing for various planets such as Mercury, Venus, Jupiter, and Saturn. This presentation will show the results of Hisaki's observation especially about Jupiter's magnetosphere.

1. Introduction

Jupiter's magnetosphere contains ultra-relativistic electrons in its radiation belt. These high energy particles are thought to be partly accelerated through the resonance effect with whistler-mode waves which is excited by anisotropic hot electrons injected from the outer magnetosphere [2]. However, radial electron transportation in the inner magnetosphere around the Io plasma torus is not well understood. The detailed observation was needed.

2. The Hisaki/EXCEED data

The only instrument on board the Hisaki is "EXCEED" which is the extreme ultraviolet (EUV) spectrometer with its spectral coverage of 52-148 nm [3, 4]. The data consists of 1-dimentional spatial information and the spectral dispersion, respectively. Figure 1 shows the EUV spectrum taken by EXCEED with its high-resolution mode. The total integration period is 550 minutes. We can see many lines from sulfur and oxygen ions in the torus. The foreground emission from geocoronal hydrogen, helium and oxygen are also shown. The spectrum fitting analysis are used to deduce the radial profile of plasma parameters such as the electron density, temperature, and ion compositions. According to the analysis, we show evidence for global inward transport of flux tubes containing hot plasma [5]. Other than high-resolution mode, the observation with full latitudinal coverage of Io plasma torus was continued for more than 3 months. The emissions from the Io plasma torus and Jupiter's northern aurora were monitored continuously (every ~50 minutes per orbit) [6].

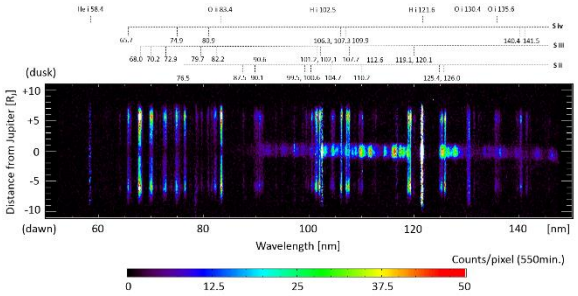

Figure 1: EUV spectrum from Io plasma torus taken by EXCEED on Hisaki (from reference 5). The horizontal axis means spectral dispersion and the vertical axis shows spatial distribution.

3. Conclusion

The EUV spectrum from Io plasma torus and Jupiter's aurora taken by Hisaki were analyzed. The radial variations of plasma parameters and temporal modulations of Io plasma torus and Jupiter's aurora were deduced.

Acknowledgements

The authors thank all the members of Hisaki/SPRINT-A mission. This research was supported by a grant-in-aid for Scientific Research from the Japan Society for the Promotion of Science (JSPS).

References

[1] Yoshikawa, I. et al.: Extreme ultraviolet radiation measurement for planetary atmospheres/magnetospheres from the earth-orbiting spacecraft (EXCEED), Space Sci. Rev., 184, 237–258, DOI: 10.1007/s11214-014-0077-z, 2014.

[2] Horne, R. et al.: Gyro-resonant electron acceleration at Jupiter, Nature Phys., 4, 301–304, DOI: 10.1038/nphys897, 2008.

[3] Yamazaki, A. et al.: Field-of-View Guiding Camera on the HISAKI (SPRINT-A) Satellite, Space Sci. Rev., 184, 259–274, DOI: 10.1007/s11214-014-0106-y, 2014.

[3] Yoshioka, K.: The extreme ultraviolet spectroscope for planetary science, EXCEED, Planet. Spa. Sci., 85, 250-260, DOI: 10.1016/j.pss.2013.06.021, 2013.

[5] Yoshioka, K. et al.: Evidence for global electron transportation into the jovian inner magnetosphere, Science, 345, 1581–1584, DOI: 10.1126/science.1256259, 2014.

[6] Kimura, T. et al.: Transient internally driven aurora at Jupiter discovered by Hisaki and the Hubble Space Telescope, Geophys. Res. Let., 42, DOI: 10.1002/2015GL063272, 2015.

EPSC Abstracts
Vol. 10, EPSC2015-179, 2015
European Planetary Science Congress 2015

Magnetic reconnection in Saturn's magnetotail: A comprehensive magnetic field survey.

A. W. Smith (1), C. M. Jackman (1), M. F. Thomsen (2), and M. K. Dougherty (3)

(1) Department of Physics & Astronomy, University of Southampton, Southampton, UK (AW.Smith@soton.ac.uk), (2) Planetary Science Institute, Tucson, Arizona, USA, (3) Department of Physics, Imperial College London, London, UK

Abstract

Magnetic reconnection is a fundamental process throughout the solar system, significantly shaping and modulating the magnetospheres of the magnetized planets. Within planetary magnetotails reconnection can be responsible for energizing particles and potentially changing the total flux and mass contained within the magnetosphere. The Kronian magnetosphere is thought to be a middle ground between the rotationally dominated Jovian magnetosphere and the solar wind driven terrestrial magnetosphere. However, previous studies have not been able to find a statistical reconnection x-line, as has been possible at both Jupiter and Earth. Additionally the standard picture of magnetotail reconnection at Saturn, developed by Cowley et al. [2004], suggests a potential asymmetry between the dawn and dusk flanks, caused by different reconnection processes dominating.

This work centers on the development of an algorithm designed to find reconnection related events in spacecraft magnetometer data, aiming to reduce the bias that manual searches could inherently introduce, thereby ensuring the validity of any statistical analysis. The algorithm primarily identifies the reconnection related events from deflections in the north-south component of the magnetic field, allowing an almost uninterrupted in-situ search (when the spacecraft is situated within the magnetotail).

The new catalogue of candidate reconnection events, produced by the algorithm, enables a more complete statistical view of reconnection in the Kronian magnetotail. Well-studied data encompassing the deep magnetotail and dawn flank (particularly from orbits in 2006) were used to train the algorithm and develop reasonable criteria. The algorithm was then applied to data encompassing the dusk flank (including orbits from 2009, for which plasma data have been examined by Thomsen et al. [2014]). This combination enables a robust, and global, comparison of reconnection rates, signatures and properties in the Kronian magnetotail.

EPSC Abstracts
Vol. 10, EPSC2015-306, 2015
European Planetary Science Congress 2015

On the nature of MHD and kinetic scale turbulence in the magnetosheath of Saturn: Cassini observations

L. Hadid (1), F. Sahraoui (1), K. H. Kiyani (1), A. Retinó(1), R. Modolo, (2), P.Canu (1), A. Masters(3), and M. Dougherty(3).
(1) Laboratoire de Physique des Plasmas, Observatoire de Saint-Maur, Saint-Maur-Des-Fossés, 94107 France, (2)LATMOS, CNRS-UVSQ-UPMCS, Guyancourt, France, (3) Imperial College, United Kingdom.
(lina.hadid@lpp.polytechnique.fr)

Abstract

Low frequency turbulence in Saturn's magnetosheath is investigated using in-situ measurements of the Cassini spacecraft. We focus on the magnetic energy spectra computed in the frequency range $\sim [10^{-4}, 1]$Hz. Three main results are reported: 1) The magnetic energy spectra showed a $\sim f^{-1}$ scaling at MHD scales followed by an $\sim f^{-2.6}$ scaling at the sub-ion scales without forming the so-called inertial range, breaking the universality of the Kolmogorov spectrum in the magnetosheath; 2) The magnetic compressibility and the cross-correlation between the parallel component of the magnetic field and density fluctuations $C(\delta n, \delta B_{||})$ indicate the dominance of the compressible magnetosonic slow modes at MHD scales rather than the Alfvén mode [3] ; 3) Higher order statistics revealed a monofractal (resp. multifractal) behaviour of the turbulent flow behind a quasi-perpendicular (resp. quasi-parallel) shock at the sub-ion scales.

1. Introduction

In order to expand our knowledge in plasma turbulence and thanks to the Cassini spacecraft mission, we decided to explore the properties of turbulence in the Kronian magnetosheath. These properties include the magnetic field energy spectra, the magnetic compressibility and intermittency, at both MHD and kinetic scales (Not shown here)

2. Observations and results

The analysis is based on in-situ data provided by the Fluxgate Magnetometer of the MAG instrument [1], which measures the magnetic field data with 32ms time resolution and the plasma data from the CAPS/IMS (Cassini PlasmaSpectrometer) and the Electron Spectrometer (ELS) [5], during 39 shock-crossings between 2004 and 2005. Similarities and differences were found between the different media, in particular about the nature of the turbulence and its scaling laws.

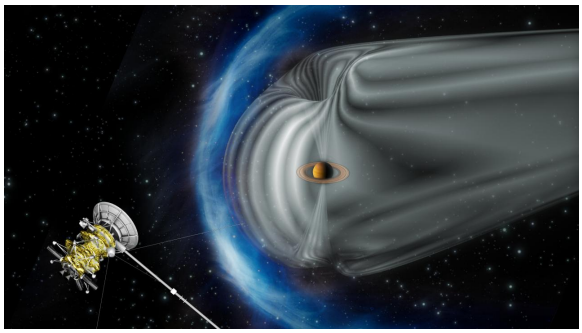

Figure 1: Saturn's magnetosphere is depicted in grey, while the shock wave in the solar wind that surrounds the magnetosphere is shown in blue. The image is not to scale.
Credit: ESA.

2.1. Power Desnity Spectra

We first computed the power density spectra of the interplanetary magnetic fluctuations measured for a set of 39 magnetosheath crossings as have been cited earlier. As we can see from figure 2, we found that the spectra are different from those measured in the solar wind: the MHD scales show a $\sim f^{-1.26}$ spectrum rather than the Kolmogorov scaling f -5/3. And at the sub-ion scales ($f < 10^{-2}$Hz) the spectra steepen to $\sim f^{-2.6}$ similarly to previous observations in the terrestrial magnetosheath or the solar wind at 1AU [Sahraoui et al., ApJ, 2013].

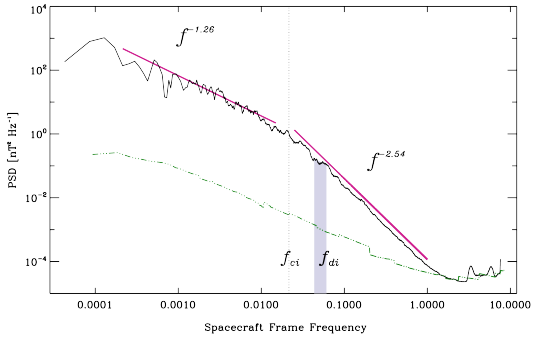

Figure 2: δB power spectral density for the analyzed time interval measured between 03:00-08:00.

2.2. Wave Modes propagation

To identify the nature of plasma modes that carry the energy cascade from the "energy-containing scales" to the sub-ion ones, we use the magnetic compressibility C_B defined as:

$$C_B(f) = \frac{|\delta B_{\parallel}(f)|^2}{|\delta B(f)|^2} \quad (1)$$

Figure 3 shows an example of the measured magnetic compressibility. One can see a relatively constant and high magnetic compressibility $C_B > 1/3$, which indicates the dominance of the parallel component $\delta B_{\parallel}$. This clearly rules out the Alfvénic fluctuations as a dominant component of the turbulence at least at MHD scales ($f < f_{ci} \sim 0.05$Hz). Studying as well the cross correlation between the magnetic field and the electron density fluctuations $C(\delta B_{||}, \delta n_e)$. We found that that locally and on average the density and the parallel component of the magnetic fluctuations are anti-correlated, i.e. $C(\delta B_{||}, \delta n_e) < 0$. This cleary rules out the fast mode fluctuation as the dominant component of the turbulence.

2.3. Higher Order Statistical study

To investigate the mono-fractal versus multi-fractal nature of the observed turbulence at MHD and sub-ion scales we analyze the Probability Density Function (PDF) of the magnetic field temporal increments and the structure functions at different orders. We find that at sub-ion scales, behind a quasi-perpendicular bow shock the turbulence is random like and self-similar however behind a quasi-parallel bowshock the fluctuations are intermittent

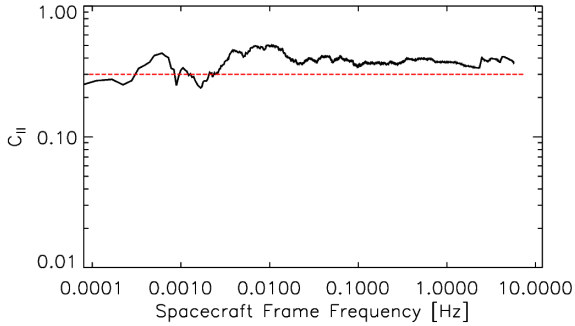

Figure 3: Magnetic compressibility of the magnetic field fluctuations.

3. Summary and Conclusions

Thanks to analyzing sufficiently long and relatively stationary time series measured by the Cassini spacecraft in the magnetosheath of Saturn away from the flanks we showed the absence of the Kolmogorov scaling $\sim f^{-5/3}$ at MHD scales, which scale as $\sim f^{-1}$ suggesting the random-like nature of the fluctuations, contrary to known results on the solar wind turbulence [2]. The spectra steepen above the spectral break to $\sim f^{-2.6}$. Moreover by studying the magnetic compressibility and the cross-correation between the density and the parallel magnetic field, our results suggest that turbulence in the magnetosheath of Saturn is dominated by compressible Slow magnetosonic modes.

References

[1] M.K Dougherty et al. "The Cassini Magnetic field investigation", Space Sci. Rev. 114, 331 (2004)

[2] Kiyani et al. "Enhanced magnetic compressibility and isotropic scale-invariance at sub-ion Larmor scales in solar wind turbulence" ApJ, (2013)

[3] Sahraoui et al. "Evidence of a Cascade and Dissipation of Solar-Wind Turbulence at the Electron Gyroscale", PRL, vol.102, (2009)

[4] Sahraoui et al. "New insight into short-wavelength solar wind fluctuations from Vlasov theory", ApJ, 2012

[5] Young et al. ''Cassini Plasma Spectrometer Investigation", Space Sci. Rev. Vol.114, Issue 1-4, pp 1-112 (2004)

EPSC Abstracts
Vol. 10, EPSC2015-368, 2015
European Planetary Science Congress 2015

Ion cyclotron waves at Saturn: Latitude structure and implications for the vertical extent of the neutral cloud

F. Crary, V. Dols, T. Cassidy
University of Colorado, Laboratory for Atmospheric and Space Physics, Boulder, United States (fjcrary@gmail.com)

Abstract

We present an analysis of ion cyclotron waves in Saturn's magnetosphere. Following earlier work by Leisner et al., 2011, who examined data from 11 Cassini in 2005-2006, we consider the amplitude and frequency distribution of ion cyclotron waves. We used the spacecraft's 111 inclined orbits between 2004 and 2015. Based on the vertical distribution of these waves, we infer the vertical distribution of fresh ion production and therefore the vertical distribution of Saturn's neutral cloud.

1. Introduction

Ion cyclotron waves are left-circularly polarized electromagnetic waves at or slightly below the ion cyclotron frequency. They are generated by freshly ionized particles in an unstable ring distribution. As such, they offer a tracer for the production of plasma and the distribution of neutrals in a planet's magnetosphere.

Analysis of early Cassini observations [Leisner et al., 2011] obtained on 11 orbits in 2005-2006, showed that ion cyclotron wave amplitudes peak off the equator and that the peak frequency was higher as the spacecraft approached the equator than after crossing the equator. This was interpreted as ion production confined to the equator, advective growth of the waves as they propagated away from the equator, and a Doppler shift in frequency due to the vertical component of the spacecraft's velocity.

2. Current analysis

Here, we expand these observations to include the 111 equator crossings between 2004 and 2015 with an inclination greater than 5o and a radius less than 10 Saturn radii. This will verify the Doppler shift interpretation and provide a statistical map of wave amplitude versus latitude and radius. These results when combined with theory and modeling of advective growth constrain the vertical extent of the source region. This will be compared with theoretical calculations of ion production based on models of the neutral cloud and its vertical extent.

References

[1] Leisner, J., S., C. T. Russell, H. Y. Wei, and M. K. Dougherty, Probing Saturn's ion cyclotron waves on high-inclination orbits: Lessons for wave generation, *J. Geophys Res., 116*, A09235, 2011.

EPSC Abstracts
Vol. 10, EPSC2015-418, 2015
European Planetary Science Congress 2015

Plasma Parameters in Io's Torus: Measurements from Apache Point Observatory

Nick Schneider (1), Jake Turner (2), Carl Schmidt (2), Michael Chaffin (1), Eric McNeil (1), Stacey Rugenski (2), Nancy Chanover (3), Apurva Oza (2), Alexander Thelen (3), Robert E. Johnson (2), Lauren Bittle (2), Patrick King (2)

(1) Laboratory for Atmospheric and Space Physics, University of Colorado, 3665 Discovery Dr., Boulder, CO 80303, (2) University of Virginia, (3) New Mexico State University (nick.schneider@lasp.colorado.edu)

Abstract

We report observations from nine nights of observations of the Io plasma torus made in conjunction with JAXA's Hisaki mission torus observations and the Hubble Space telescope auroral campaign. Groundbased remote sensing of forbidden line emissions yield measures of plasma density which cannot be made at UV wavelengths.

1. Introduction

The Io plasma torus is an astrophysical nebula wrapped around Jupiter, originating from the intense volcanic activity of Jupiter's moon Io. The torus varies both spatially and temporally, driven by changes in volcanism and asymmetries in the Jovian magnetosphere. We report results from 9 nights of observation spanning November 2013 to February 2014 with the Dual Imaging Spectrograph on the ARC 3.5m telescope at Apache Point Observatory in New Mexico. Emissions in these data include the [SII] doublets at 6716/6731A and 4069/4076A, [OII] at 3726/3729A, [SIII] at 3722A and 6312A, as well as resonantly scattered neutral [NaI] at 5890/5896A. Constraints on electron density, temperature and ion mixing rations can be obtained. Observations of both ansa during a 5 hour period characterize the complete longitudinal structure. Specifically, the intensity ratio of the collisionally excited [SII] doublet at 6716/6731A is a diagnostic for local electron density sampled at ~20 minute cadence. Absolute intensity can be derived directly from the reflectance of Jupiter's disc and standard calibrations are performed on the data such as bias subtraction, wavelength calibration and rectification. A unique background subtraction procedure is developed to disentangle scattered Jovian reflection and the torus. These observations were made in conjunction with JAXA's Hisaki mission, the HST auroral campaign and infrared monitoring of volcanism to better understand how mass and energy are transported throughout the system.

2. Figures

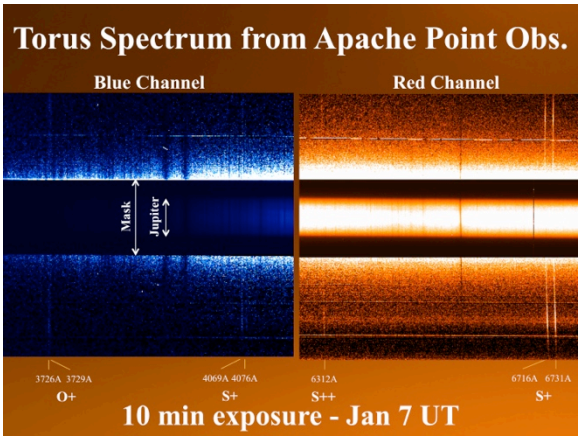

Figure 1: Visible wavelength spatially-resolved spectrum of the Io plasma torus, showing emissions from S^{+}, S^{++} and O^{+}. Sky subtraction and image rectification have not yet been performed on this dataset. The slit spans both sides of the plasma torus (shown vertically); Jupiter's spectral image lies across the image center. It was obtained through a neutral density filter to reduce stray light within the instrument. The Jupiter spectral image provides spatial registration and intensity calibration. Multiple images were obtained during one observing sessions, allowing plasma properties of the torus to be derived as a function of longitude around Jupiter and independently on the east (dawn) and west (dusk) sides of Jupiter.

EPSC Abstracts
Vol. 10, EPSC2015-484, 2015
European Planetary Science Congress 2015

Statistical analysis and multi-instrument overview of the quasi-periodic 1-hour pulsations in Saturn's outer magnetosphere

B. Palmaerts (1,2), E. Roussos (1), N. Krupp (1), W. S. Kurth (3), D. G. Mitchell (4) and M. K. Dougherty (5)
(1) Max-Planck-Institute für Sonnensystemforschung, Göttingen, Germany, (2) Laboratoire de Physique Atmosphérique et Planétaire, Université de Liège, Liège, Belgium, (3) Department of Physics and Astronomy, University of Iowa, Iowa City, IA 52242-1479, USA, (4) Johns Hopkins University Applied Physics Laboratory, Laurel, MD 20723, USA, (5) Space and Atmospheric Physics, The Blackett Laboratory, Imperial College London, London SW7 2AZ, UK (palmaerts@mps.mpg.de)

Abstract

The in-situ exploration of the magnetospheres of Jupiter and Saturn has revealed different periodic processes. In particular, in the Saturnian magnetosphere, several studies have reported pulsations in the outer magnetosphere with a periodicity of about 1 hour in the measurements of charged particle fluxes, plasma wave, magnetic field strength and auroral emissions brightness. The Low-Energy Magnetospheric Measurement System detector of the Magnetospheric Imaging Instrument (MIMI/LEMMS) on board Cassini regularly detects 1-hour quasi-periodic enhancements in the intensities of electrons with an energy range from a hundred keV to several MeV.

We extend an earlier survey of these relativistic electron injections, using 10 years of LEMMS observations in addition to context measurements by several other Cassini magnetospheric experiments. During this period, we identified 720 pulsed events in the outer magnetosphere over a wide range of latitudes and local times, revealing that this phenomenon is common and frequent in Saturn's magnetosphere. However, the distribution of the injection events presents a strong local time asymmetry with ten times more events in the duskside than in the dawnside. In addition to the study of their topology, we present a first statistical analysis of these pulsed events to investigate their properties. This analysis reveals that the mean interpulse period is 68 ± 10 minutes and that the events are made up of less than 9 pulses in general, but they can include up to 19 pulses. The most common shape of these pulses is a fast rise followed by a slow decay. Moreover, the ratio between the rise rate and the decay rate increases with the energy.

We have also investigated the signatures of each electron injection event in the observations acquired by the Radio and Plasma Wave Science (RPWS) instrument and the magnetometer (MAG). Correlated pulsed signatures are observed in the plasma wave emissions, especially in the auroral hiss, for 12% of the electron injections identified in the LEMMS data. Additionally, in about 20% of the events, such coincident pulsed signatures have been also observed in the magnetic field measurements, some of them being indicative of field-aligned currents. This multi-instrument approach sets constraints on the origin and significance of the pulsed events.

EPSC Abstracts
Vol. 10, EPSC2015-512, 2015
European Planetary Science Congress 2015

Case study of quasi-steady reconnection in Saturn's magnetotail, and update on our current understanding of mass transport and loss in Saturn's nightside magnetosphere

C.M. Jackman (1), M.F. Thomsen (2), D.G. Mitchell (3), N. Sergis (4), C.S. Arridge (5), M. Felici (6,7,5), S.V. Badman (5), C. Paranicas (3), X. Jia (8), G.B. Hospodarksy (9), M. Andriopoulou (10), K.K. Khurana (11), A.W. Smith (1), M.K. Dougherty (12)
(1) University of Southampton, Southampton, UK, (2) Planetary Science Institute, Tucson, AZ, USA (3) Johns Hopkins University Applied Physics Laboratory, Laurel, MD, USA (4) Academy of Athens, Athens, Greece, (5) Department of Physics, Lancaster University, Lancaster, UK, (6) Mullard Space Science Laboratory, University College London, Surrey, UK, (7) The Centre for Planetary Sciences at UCL/Birkbeck, London, UK, (8) University of Michigan, Ann Arbor, MI, USA, (9) Department of Physics and Astronomy, University of Iowa, Iowa City, Iowa, USA, (10) Space Research Institute, Austrian Academy of Sciences, Graz, Austria, (11) Institute of Geophysics and Planetary Physics, University of California at Los Angeles, LA, CA, USA, (12) Blackett Laboratory, Imperial College London, Prince Consort Road, London, UK. (c.jackman@soton.ac.uk)

Abstract

We present a case study of an event from August 20th (day 232) of 2006, as viewed by magnetic field, plasma, energetic particle and plasma wave sensors (MAG/CAPS/MIMI/RPWS) when the Cassini spacecraft was sampling the region near 32 Rs and 22 hours LT in Saturn's magnetotail. Cassini observed a strong northward-to-southward turning of the magnetic field, which is interpreted as the signature of dipolarization of the field as seen by the spacecraft planetward of the reconnection x-line. This event was accompanied by very rapid (up to ~1500 km s^{-1}) thermal plasma flow toward the planet. At energies above 28 keV, energetic hydrogen and oxygen ion flow bursts were observed to stream planetward from a reconnection site downtail of the spacecraft. Meanwhile a strong field-aligned beam of energetic hydrogen was also observed to stream tailward, likely from an ionospheric source. Saturn Kilometric Radiation emissions were stimulated shortly after the observation of the dipolarization. We discuss the field, plasma, energetic particle and radio observations in the context of the impact this reconnection event had on global magnetospheric dynamics.
We also discuss this event in terms of other recent studies of reconnection in Saturn's tail and update on the emerging picture concerning our understanding of how mass is transported and lost within Saturn's magnetosphere.

EPSC Abstracts
Vol. 10, EPSC2015-708, 2015
European Planetary Science Congress 2015

Influence of B_y and B_z interplanetary magnetic field components on planetary magnetopause position and shape: qualitative analysis and comparison with modelling and observation results

M.I. Verigin, G.A. Kotova, V.V. Bezrukikh, and A.P. Remizov
Space Research Institute of Russian Academy of Sciences, Profsoyuznaya, 84/32, Moscow, 117997, Russia
(verigin@iki.rssi.ru)

Abstract

Interplanetary magnetic field (IMF) B_y and B_z components influence on planetary magnetopause position and shape in two different ways: (i) presence of both components generally leads to increase of total pressure near the magnetosheath flow stagnation point and (ii) B_z part of IMF additionally leads to variation of the magnetopause shape. Both effects are qualitatively considered in the talk.

1. Introduction

It is generally valid that the solar wind ram pressure ρV^2 is the main factor contributing into the magnetopause stagnation pressure which can be approximated then as $\Pi \approx k\rho V^2$ with k being a function of solar wind specific heat ratio γ and sonic Mach number M_s :

$$k = \frac{1}{\gamma}\left(\frac{\gamma+1}{2}\right)^{(\gamma+1)/(\gamma-1)}\left(\gamma - \frac{\gamma-1}{2M_s^2}\right)^{1/(1-\gamma)}. \quad (1)$$

Complementary factors that are influencing on magnetopause position and shape are: (i) magnetic field line tension resulting in the clock angle dependency of the magnetopause terminator cross-section [1], (ii) magnetic field pressure leading to magnetopause movement towards the Earth when the IMF cone angle approaching π/2 [2], and (iii) IMF B_z component increasing magnetopause nose bluntness for southward B_z direction [3]. It was shown [4] that the contribution of the magnetic field line tension to the stagnation pressure is ~ $2\Delta/R$ times less than contribution of the magnetic pressure itself, where Δ is the magnetosheath thickness and R is the magnetic field lines curvature radius. Thus field line tension effects will be omitted in subsequent analysis.

2. Basic approach and relations

Empiric relations for the description of the total Π, thermal P_{th}, and magnetic field P_{mag} pressures at the magnetopause nose are based on results of 3-D MHD modelling [5] and analytic solutions in Lagrangian variables [6]:

$$\Pi = k\rho V^2 \cdot \left(1 + \left(\frac{\sqrt{6}\cdot Sin^2\vartheta_{bv}}{M_a^2}\right)^{2/3}\right), \quad (2)$$

$$P_{th} = k\rho V^2 \Big/ \left(1 + 25\sqrt{\frac{Sin^2\vartheta_{bv}}{M_a^2}}\left(2 - \sqrt{\frac{6}{M_s}}\right)\right), \quad (3)$$

$$P_{mag} = \Pi - P_{th}, \quad (4)$$

where M_a is Alvenic Mach number and ϑ_{bv} is the angle between solar wind and IMF directions. Figure 1 presents correspondence of relations (2 - 4) to results of 3-D MHD modelling [5].

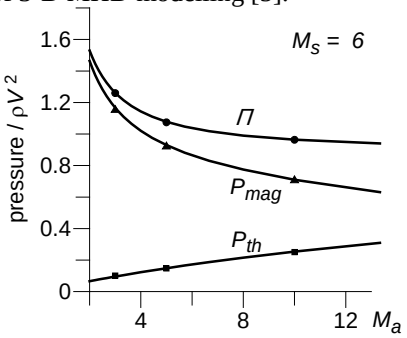

Figure 1. Comparison of 3-D MHD calculations with approximating relations (2 - 4).

The next important relation (5) of our approach comes from so called 'doubling factor' f_d that indicate how much the internal magnetosperic field is increased in the subsolar region due to

Chapman-Ferraro currents. With the use of ellipsoidal model by Tsyganenko [7] we approximated f_d by the following relation :

$$f_d = 2 + \exp\left(-\frac{5}{3}\left(\frac{R_0}{r_0} - 1\right)\right), \qquad (5)$$

where r_o and R_o are the planetocentric distance to the magnetopause nose and its curvature radius. Figure 2 presents correspondence of relation (5) to results of model [7].

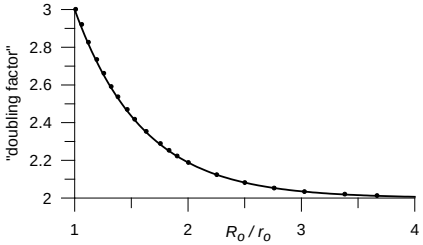

Figure 2. Comparison of Tsyganenko model [7] results (dots) with calculations by the expression (5).

Additional basic relation of the model (adjusted by comparison of resultant model with observations) describes the increase of the ratio R_o / r_o in (5) with increase of southward IMF B_z component that provides more blunt magnetosphere nose for the southward IMF.

3. Summary and Conclusions

Incorporation of theoretically background relations (2 - 5) into magnetopause model (e.g. in [1]) provides possibility to describe variation of the magnetopause position and shape for wide range of solar wind ram pressures and IMF B_y and B_z components.

Qualitatively, increase of either northward or southward IMF B_z component leads to the increase of total magnetosheath pressure at the stagnation point (see relation (2)) thus suggesting magnetopause motion to the planet. On the other hand, the dependence of the magnetopause shape R_o / r_o and 'doubling factor' (5) on IMF B_z component provides "blunted" magnetopause for southward IMF and "sharpened" magnetopause for northward IMF. Decreased 'doubling factor' (5) for southward IMF leads to "rapid" approach of "blunted" magnetopause to the Earth while increased f_d for northward IMF provides "stagnative" behavior of the "sharpened" magnetopause with increase of northward component of IMF, that qualitatively corresponds to magnetopause observations (see, e.g., [3]).

Acknowledgements

The paper is partially supported by the program P9 of RAS.

References

[1] M.I. Verigin, G.A. Kotova, V.V. Bezrukikh, G.N. Zastenker, and N. Nikolaeva: Analytical Model of the Near_Earth Magnetopause According to the Data of the Prognoz and Interball Satellite Data, *Geomagn. and Aeronomy*, 49, No. 8, 1176–1181, 2009.

[2] Dušík, Š., G. Granko, J. Šafránková, Z. Němeček, and K. Jelínek: IMF cone angle control of the magnetopause location: Statistical study, *Geophys. Res. Lett.*, 37, L19103, doi:10.1029/2010GL044965, 2010.

[3] D.G. Sibeck, R.E Lopez, R.C. Roelof: Solar Wind Control of the Magnetopause Sape, Location, and Motionm, *J. Geophys. Res.*, 96, No.A4, 5489-5495б 1991 .

[4] M. Verigin, M. Tatrallyay, G. Erdos, G. Kotova, V. Bezrukikh, A. Remizov: The influence of magnetosheath magnetic field line stress and pressure on the geomagnetopause position and shape, *The 40-th COSPAR Scientific Assembly*, 2-10 Aug. 2014, Moscow, Russia, Abstract D3.5-0014-14, 2014.

[5] S.S. Stahara: Adventures in the magnetosheath: two decades of modeling and planetary applications of the Spreiter magnetosheath model, *Planet. and Space Sci.*, 50, 421 -442, 2002.

[6] F.V. Shugaev, A.P. Kalinchenko, Reflection of fast magnetosonic wave from the front of a fast MHD shock wave, Proceedings of the 15 International Conference on MHD Energy Conversion and the 6 International Workshop on Magnetoplasma Aerodynamics, ed.by V.A. Bityurin, Moscow IVTAN, Vol.2, ph.617-620, 2005.

[7] N.A. Tsyganenko: A solution of the Chapman-Ferraro problem for an ellipsoidal magnetopause, Planet. and Space Sci., 37, No.9, 1037–1046, 1989.

EPSC Abstracts
Vol. 10, EPSC2015-723-2, 2015
European Planetary Science Congress 2015

Electron impact ionization in Titan's sunlit ionosphere

E. Vigren (1), M. Galand (2), A. Wellbrock (3), A. J. Coates (3), N. J. T. Edberg (1), J.-E. Wahlund(1), P. Lavvas (4), V. Vuitton (5), and J. Cui (6)

(1) Swedish Institute of Space Physics, Uppsala, Sweden (erik.vigren@irfu.se), (2) Department of Physics, Imperial College London, London, UK, (3) Mullard Space Science Laboratory, University College London, Surrey, UK, (4) Université Reims Champagne-Ardenne, Reims, France, (5) Univ. Grenoble Alpes, CNRS, IPAG, Grenoble, France. (6) Key Laboratory of Lunar and Deep Space Exploration, Chinese Academy of Sciences, Beijing, China.

Abstract

Solar EUV driven model calculations of the thermal electron balance in Titan's sunlit ionosphere overestimate the Langmuir probe derived electron number densities by a factor of ~2 [1]. Whether the cause of the discrepancy is overestimated plasma production, underestimated plasma loss or a combination of the two is an open question. In the present work we show and discuss comparisons of model derived suprathermal electron intensities with CAPS/ELS [2] spectra in Titan's sunlit ionosphere (focusing on the T40-T42 and T48 Titan flybys by the Cassini spacecraft). The model accounts only for photoelectrons and associated secondary electrons with the main input being the impinging solar EUV spectrum at the day of the investigated flybys, as measured by TIMED/SEE (Level 3) [3] and extrapolated to Saturn. Associated electron impact ionization rates have been derived by integrating the electron intensities over energy, invoking the ambient number densities of N_2 and CH_4, and the related energy dependent electron-impact ionization cross sections. Focusing on the altitude regime 1000-1200 km the electron impact ionization rates derived with modeled intensities are on average ~80% higher than values derived with CAPS/ELS based intensities. This is counter-intuitive and potential reasons will be discussed. The results indicate that overestimated plasma production through photoionization *possibly* contributes to the present difficulties in accurately reproducing number densities of free thermal electrons in Titan's main sunlit ionosphere. This requires, however, further studies to be confirmed or dismissed.

References

[1] Vigren, E., et al.: On the thermal electron balance in Titan's sunlit ionosphere, Icarus, 223, 234.

[2] Wellbrock, A., et al: Cassini observations of ionospheric photoelectrons at large distances from Titan: Implications for Titan's exospheric environment and magnetic tail, JGR, 117, A03216.

[3] Woods, T. N., et al: Solar EUV Experiment (SEE): Mission overview and first results, JGR, 110, A01312.

EPSC Abstracts
Vol. 10, EPSC2015-818, 2015
European Planetary Science Congress 2015

A Statistical Study of Wave Activity in the Hermian Magnetosphere.

M. K. James, E. J. Bunce, T. K. Yeoman and S. M. Imber
Radio and Space Plasma Physics Group, University of Leicester, UK (mkj13@le.ac.uk)

Abstract

A statistical study of wave activity within the Hermian magnetosphere is undertaken using data obtained from the MESSENGER mission between March 2011 and March 2014. Wave activity is categorised by its predominant polarisation - allowing for the comparison between compressional wave events and those more Alfvénic in nature. The position of the spacecraft at the time of each spectrum is mapped both to the magnetic equatorial plane, and the planetary surface at Mercury in order to determine the location of each wave event within the magnetosphere.

1. Introduction

Wave activity is commonly observed within Mercury's magnetosphere (e.g. [1, 2]) using magnetic field data. Small amplitude, narrow bandwidth ULF waves observed by Mariner 10 in 1974 were suggested to be caused by a resonant interaction, driving standing waves on field lines possibly anchored to the planet's core [1]. As the wave frequencies often lie between the gyrofrequencies of protons and sodium ions, an alternative explanation for this wave activity is a hybrid resonance in a plasma with more than one significant component species (e.g. [3, 4]).

A recent survey of ULF waves at Mercury [2] searched MESSENGER magnetometer data between March 2011 and September 2011 for wave activity in the inner magnetosphere. This study observed maximum wave power near the equator of Mercury, suggesting a that the source of some of the wave activity observed lies in the equatorial plane. Polarisation analysis of these waves found evidence for ion cyclotron waves, compressional events and possible field line resonances.

This study performs a search for ULF wave activity in the MESSENGER magnetometer data between March 2011 and March 2014 with the aim of characterising wave activity in different regions of the magnetosphere, elucidating the source mechanisms responsible and examining the properties of the plasma in the vicinity of the waves.

2. Data Analysis

The parallel, $\mathbf{B}_{||}$, and radial, $\mathbf{B}_r$, components of the magnetic field were combined to form an overall compressional component, for direct comparison with the azimuthal, $\mathbf{B}_\phi$, component associated with Alfvénic wave activity. Fourier analysis was performed on both components using a 60 s sliding window where a peak detection algorithm searched for waves present in the data. A ratio, R, is defined by comparing the Fourier power of the two components, where $0 \leq R < 1$ indicates a compressionally dominant wave and $R > 1$ is azimuthally dominant.

3. Results

Wave activity has been traced to the magnetic equatorial plane at Mercury using the paraboloid field model [5] in order to help determine types of wave activity dominating in different regions of the magnetosphere. Figure 1 shows the occurrence rate of the azimuthally dominant wave events in the $X - Y$ MSM plane. The occurrence rate of azimuthally dominant waves is highest on the flanks of the magnetosphere near dawn and dusk. A possible explanation for these wave populations is in toroidal field line resonances, potentially driven by Kelvin-Helmholtz waves on the magnetopause.

The position of the spacecraft at the time of each spectrum has been mapped onto a 1 R_M sphere centred on the magnetic dipole at Mercury using the paraboloid model [5]. Figure 2 shows the standard deviation in the frequencies observed at each bin in magnetic latitude and MLT. A region of decreased standard deviation surrounded by an increase in frequency variation on the night-side of the planet may be indicative of the location of the polar cap at Mercury. This increase in variation is likely a result of dynamics of the polar cap at Mercury - each time a spectrum is traced

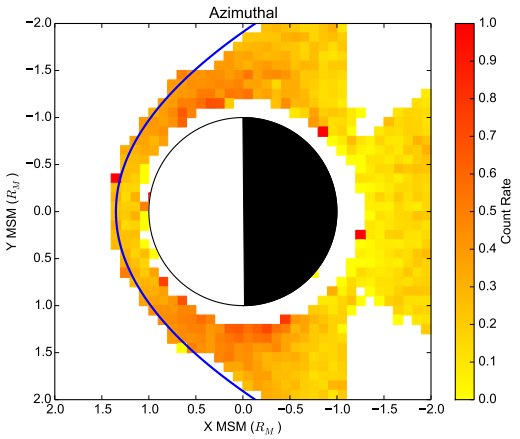

Figure 1: Occurrence rate of azimuthally oscillating waves traced to the equatorial plane.

to one of these highly variable locations, it may be in a different regime to the previous occurrence.

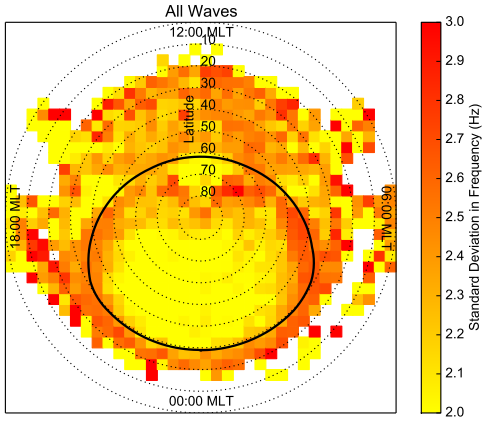

Figure 2: Standard deviation in wave frequency at the field line footprints, projected onto a 1 R_M sphere centred on the magnetic dipole, oriented such that noon is at the top and dawn to the right. The polar cap boundary found using the paraboloid field model is shown in black for comparison.

Figure 3 shows the occurrence rate of spectral peaks at various frequencies and magnetic field strengths. Between 50 and 150 nT, wave activity is commonly close the the proton cyclotron frequency (in green), suggesting that the source of many of the waves found could be related to local cyclotron resonances. Above 150 nT the activity is diverted from the proton gyrofrequency, suggesting that a different mechanism is responsible for wave generation closer to the planet.

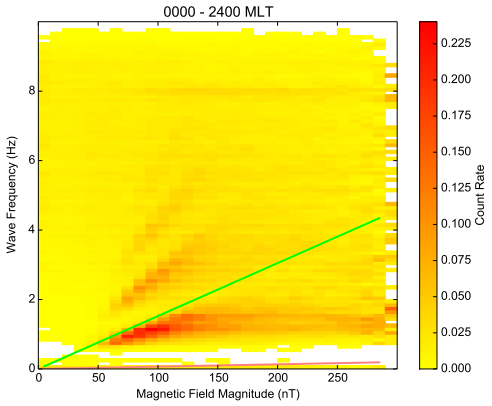

Figure 3: Occurrence rate of spectral peaks in different magnetic field strengths. Proton and sodium ion gyrofrequencies are shown in green and pink respectively.

Acknowledgements

The MESSENGER project is supported by the NASA Discovery Program under contracts NAS5–97271 to The Johns Hopkins University Applied Physics Laboratory and NASW-00002 to the Carnegie Institution of Washington.

References

[1] Russell, C. T. (1989), Ulf waves in the mercury magnetosphere, *Geophys. Res. Lett.*, *16*(11), 1253–1256, doi:10.1029/GL016i011p01253.

[2] Boardsen, S. A., J. A. Slavin, B. J. Anderson, H. Korth, D. Schriver, and S. C. Solomon (2012), Survey of coherent 1 hz waves in mercury's inner magnetosphere from messenger observations, *J. Geophys. Res.*, *117*(A12), doi:10.1029/2012JA017822.

[3] Othmer, C., K.-H. Glassmeier, and R. Cramm (1999), Concerning field line resonances in mercury's magnetosphere, *J. Geophys. Res.*, *104*(A5),10,369–10,378, doi:10.1029/1999JA900009.

[4] Klimushkin, D. Y., P. N. Mager, and K.-H. Glassmeier (2006), Axisymmetric Alfvén resonances in a multicomponent plasma at finite ion gyrofrequency, *Ann. Geophys.*, *24*(3), 1077–1084, doi:10.5194/angeo-24-1077-2006.

[5] Alexeev, I. I. and Belenkaya, E. S. and Yu. Bobrovnikov, S. and Slavin, J. A. and Sarantos, M. (2008), Paraboloid model of Mercury's magnetosphere, *J. Geophys. Res.*, *113*A12,2156–2202,doi:10.1029/2008JA013368

EPSC Abstracts
Vol. 10, EPSC2015-836, 2015
European Planetary Science Congress 2015

A survey of multi-point observations of the open-closed field line boundary by the Van Allen Probes

Paddy Dixon[1], Manuel Grande[1], Elizabeth MacDonald[2]

1 – Aberystwyth University, UK, 2 – NASA Goddard Space Flight Center, US

Abstract

We perform a survey of encounters with the open/closed field line boundary (OCB) by the Van Allen Probes (October 2012 - October 2014). The work follows on from previous work investigating the November 14th 2012 lobe entry event [Dixon & MacDonald et al, under review 2015]. Previous work using the CRRES and GOES spacecraft (e.g. Thomsen et al, 1994; Moldwin et al, 1994) found that spacecraft near geosynchronous orbit were more likely to encounter the lobe in the dawn region of the magnetosphere. During the period examined, the Van Allen Probes have had apogee which precessed through all MLTs, allowing a detailed investigation. These events are comparatively rare; we use Superposed Epoch Analysis of IMF data prior to each event to provide insight into the conditions required to make the lobe accessible to the Van Allen Probes.

1. Introduction

Spacecraft encounters with the magnetospheric lobes are characterized by a rapid decrease of particle fluxes to background levels at energies from 1 eV to 40 keV [1], followed by a rapid recovery to previous levels. A strong, stretched and tail-like field is also seen when crossing into the lobes [2], especially during times of increased geomagnetic activity and southward IMF [3].

Multiple studies [e.g. 4,5] have shown a preference for lobe encounters to occur in the morning sector of the magnetosphere, with suggested causes being an asymmetry in the rate of reconnection [4] or an unbalanced inflation of the magnetosphere on the dusk side, caused by an asymmetry in the storm time ring current [6].

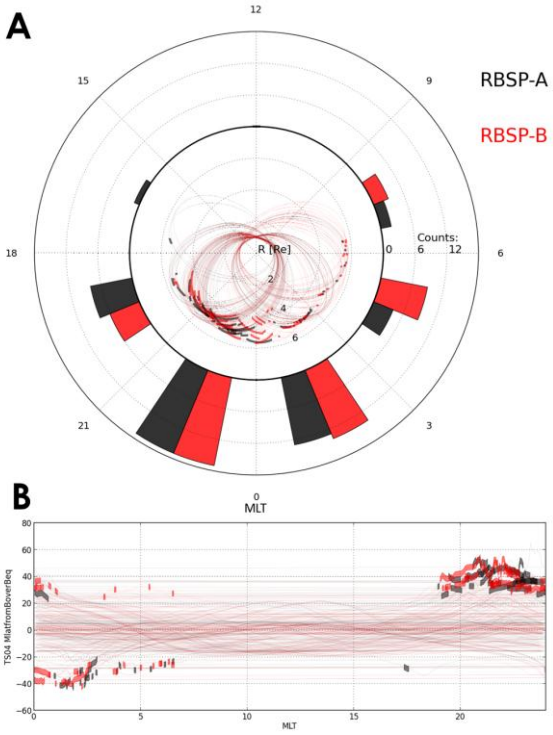

Figure 1: A) Central plot shows the orbits of the Van Allen Probes (pale lines) and the shaded boxes mark periods where the spacecraft entered the lobe. Outer plot is a histogram separated in bins of 3 MLT e.g. 0-3, 21-24 and counting the number of events that occurred in each region. B) Pale lines show the orbits of the Van Allen Probes in MLT and magnetic latitude, with shaded boxes marking periods where the spacecraft entered the lobe

2. Lobe Encounter Survey

Over a two year period (October 2012 – October 2014) the Van Allen Probes observed flux dropouts and increases in magnetic field strength consistent with crossing the open/closed field line boundary (OCB) and entering the lobe. A total of one hundred events were observed between the two spacecraft, with sixty one occurring within three hours of midnight (Figure 1).

All events occur at large magnetic latitudes - either above 20˚ in the northern hemisphere or lower than -20˚ in the southern hemisphere. There is a slight preference for dusk events, but this may be skewed

due to there being a greater number of geomagnetic storms while the Van Allen Probes had apogee in the dusk region.

3. Superposed Epoch Analysis (SEA)

Data from the EMFISIS instrument aboard the Van Allen Probes were analysed to show magnetic field characteristics as the spacecraft cross the OCB and enter the lobe. Before SEA is performed, the background magnetic field calculated using the TS04 Tsyganenko model is removed.

The signatures shown by the SEA are consistent with the spacecraft encountering a region of highly stretched magnetic field, flattened towards the x-y plane. Similar magnetic field topology was observed by the Van Allen probes for the November 14th OCB crossings [7]. As an example, one signature of this stretched field is shown for B_y in Figure 2.

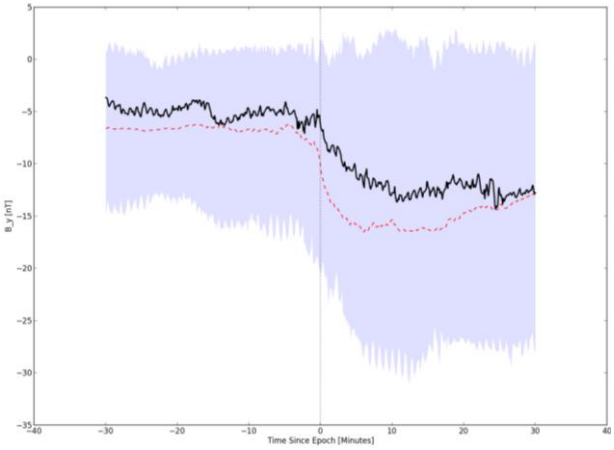

Figure 2: Superposed Epoch Analysis of B_y observations taken from the EMFISIS instrument aboard the Van Allen Probes . Epochs are defined as the start of each lobe encounter and the window size is set to thirty minutes before and after each event. The black line represents the mean, the red dashed line the median and the blue, shaded areas the limits of the upper and lower quartiles.

4. Conclusions

Over a two year period the Van Allen Probes encountered the lobe one hundred times, always at large magnetic latitudes ($> \pm 20^{\circ}$), with a slight preference for the dusk region which is possibly due to varying levels of geomagnetic activity. Fifty-one of the events were associated with a substorm injection and the majority of these events occurred near local midnight. These were most likely the result of plasma sheet thinning during the substorm growth phase.

Superposed Epoch Analysis (SEA) of the IMF conditions prior to each event show a strong signature in B_z similar to that expected for a substorm, in agreement with injections seen in the particle data. SEA of EMFISIS magnetic field data shows the spacecraft encountering a strong, highly stretched field which is consistent with lobe entry and observations of the November 14th 2012 event.

Acknowledgements

The authors would like to acknowledge the Van Allen Probes team, as well as the ECT and EMFISIS instrument teams for use of data and support. The work of P. Dixon was supported by a studentship from the Science and Technology Funding Council (STFC), UK.

References

[1] McComas, D.J., Bame, S.J., Barraclough, B.L., Donart, J.R., Elphic, R.C., Gosling, J.T., Moldwin, M.B., Moore, K.R. and Thomsen, M.F. (1993) Magnetospheric plasma analyzer: Initial three-spacecraft observations from geosynchronous orbit, *J. Geophys. Res.*, no. 98(A8), pp. 13453–13465.

[2] Fennell J., J. Roeder, H. Spence, H. Singer, A. Korth, M. Grande, A. Vampola (1996) CRRES observations of particle flux dropout events, Adv. in Space Res., 18(8), 217-228

[3] Kopányi, V. and Korth, A. (1995) 'Energetic Particle Dropouts Observed in the Morning Sector by the Geostationary Satellite GEOS-2', *Geophysical Research Letters*, no. 22, pp. 73-76, Available: DOI: 10.1029/94GL02910.

[4] Thomsen, M.F., S. J. Bame, D. J. McComas, M.B. Moldwin, and K.R. Moore (1994) The magnetospheric lobe at geosynchronous orbit, J. Geophys. Res., 99(A9), 17283-17293

[5] Moldwin, M.B., M.F. Thomsen, S. J. Bame, D. J. McComas, J. Birn, G. D. Reeves, R. Nemsek and R. D. Belian (1995), Flux dropouts of plasma and energetic particles at geosynchronous orbit during large geomagnetic storms: Entry into the lobes, J. Geophys. Res., 100(A5), 8031-8043

[6] McComas D.J., R.C. Elphic, M.B. Moldwin, M.F. Thomsen (1994), Plasma observations of magnetopause crossings at geosynchronous orbit, J. Geophys. Res., 99(A11), 21249-21255

[7] Dixon, P., MacDonald, E.A., Funsten, H.O., Glocer, A., Grande, M., Kletzing, C., Larsen, B.A. , Reeves, G. Skoug, R.M., Spence, H., Thomsen, M.F. (2015) Multipoint observations of the open-closed field line boundary as observed by the Van Allen Probes and geostationary satellites during the November 14th 2012 geomagnetic storm, J. Geophys. Res. (under review)

EPSC Abstracts
Vol. 10, EPSC2015-869, 2015
European Planetary Science Congress 2015

Ganymede's Ocean-Magnetosphere interaction and Ionosphere response

M. Ben Slama, I. Mueller-Wodarg.
Imperial College London, London, United Kingdoms

(m.benslama09@imperial.ac.uk)

Abstract

The effect of a possible ocean on Ganymede and Europa is predicted to induce a magnetic dipole as a result of the varying background magnetic field of Jupiter's magnetosphere. The case for an ocean was made by the Galileo magnetometer [3], and recently strengthened via a study using Hubble observations [4]. We investigate the effect of magnetic perturbations via both external and internal drivers. By solving the Laplace tidal equations to determine basic ocean flows as per Tyler [5] and solving the magnetic diffusion equation, we find that tides may produce magnetic perturbations at the orbital period, with amplitudes of up to ~5 nT, comparable to the externally induced magnetic perturbations at the same period. These are associated with density and electric perturbations modulated by the conductivities in the ionospheric medium.

1. Introduction

In the moons' frames of reference, the tilt in Jupiter's magnetic axis produces, via the planet's rotation, large variations in the background magnetic field. The moons' motions along their weakly eccentric orbits, which at times also cross the hinging Jovian current sheet, also cause smaller variations in the magnetic field.

The response from the ocean to these external field perturbations is investigated and modeled as a simple spherical layer with given thickness and conductivity. As per Seufert et al. [1], the response is a magnetic dipole directed along the variable external magnetic field. Its amplitude varies for different values of conductivity and thickness, and the effect of these parameters on the large-scale electric field are studied.

These studies consider the ocean as a static conductive layer, neglecting the advective effect in the diffusion equation. Here, we investigate the capability of simple ocean flows to produce weak magnetic perturbations. Propagation of ocean signals through the Ionosphere is highly sensitive to the electrical conductivities in the medium, and we determine how a satellite orbiting at, or close to the ionospheric region might detect these signals.

2. Methodology

Externally induced signals are determined following the method of Seufert et al. [1]: variability of the background magnetic field is found by fitting the moon's orbit in a Jovian magnetosphere model. At the orbital period, and for an infinitely conductive ocean at 150km depth, the induced dipole has an amplitude of ~1nT.

In order to determine tidal flow, we solve the Tidal Laplace Equations (TLE) using the time-varying gravitational potential at Ganymede's surface as the driving force. This produces perturbations in the equilibrium sea-surface height. Three sources are identified: radial and librational (due to orbit eccentricity), and obliquity (due to orbit tilt) driven tides.

These serve to amplify the natural oscillatory modes in the ocean, producing some resonance. The normal Eigen-modes of the TLE are found numerically as in [2], and resonance calculated for various ocean parameters (depth, thickness). Flow amplitudes found at Ganymede reach unexpectedly large values, comparable to Europa's [5], despite the much weaker gravitational variations.

The large intrinsic dipole field proves to be an excellent background for induction by advection: magnetic perturbations are determined by solving the

diffusion equation for a moving conductive object assuming a steady background magnetic field.

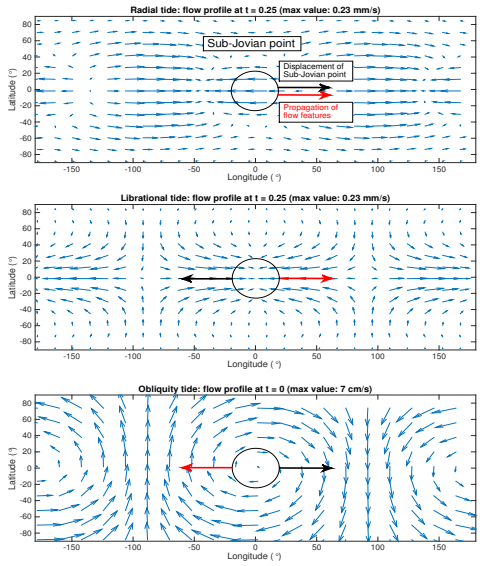

Several simplifying assumptions are made concerning the ocean: both thickness and conductivity are considered homogenous, and flow behaviour is not affected by the upper ice layer. The latter assumption will overestimate the magnitude of the flow and will be accounted for in later work.

3. Summary and Conclusions

Under the above assumptions, both externally and internally induced magnetic fields at the orbital period (171h) are of the order of a few nT (5 nT for flow induced perturbations, and 1 nT for externally induced perturbations), with dependencies on ocean conductivity and depth.

Ocean thickness was assumed to be 100km at 150km depth, while conductivity was assumed infinite. The assumption that the conductivity is large enough to produce a large response is justified in that previous works [1][3] have determined an almost 100% response at the 11h period. While at the larger 171h the response may be reduced, we expect it to remain of the same order of magnitude. We note that while both signals have the same period, their geometry is different, and their direction of propagation is opposite (tidally driven perturbations propagate westwards as opposed to eastwards for the externally induced dipole).

Further out in the ionosphere, our calculations show that the extremely low Pedersen and Hall conductivities do not affect ocean induced signals much, but allows for large (~4-7 mV/m) electric fields that may be detectable by the JUICE RPWI instrument.

Acknowledgements

MBS is funded by a studentship from the UK Science and Technology Facilities Council (STFC).

References

[1] Seufert et al.: Multi-frequency electromagnetic sounding of the Galilean moons, Icarus, 214, 477-494, 2011.

[2] Longuet-Higgins, M.S, The Eigenfunctions of Laplace's Tidal Equations over a Sphere, Phil. Trans. Of the R. Soc. of London, Math. and Phys. Science. 262, 511-607.

[3] Kivelson, M. G.; Khurana, K.; Volwerk, M.: The permanent and Inductive Magnetic Moments of Ganymede, Icarus, Vol. 157, pp. 507-522, 2002.

[4] Saur, J. et al.: The search for a Subsurface Ocean in Ganymede with Hubble Space Telescope Observations of its Auroral Ovals, J. Geophys. Res. Space Physics, 120, 1715-1737 2002.

[5] Tyler, H.: Magnetic remote sensing of Europa's ocean tides, Icarus, 211, 906-908, 2011.